ULTRASONIC VIRTUAL SOURCE IMAGING BASE ON ADAPTIVE BI-DIRECTIONAL POINT-WISE FOCUSING

Wen-tao WU [1, 2*] Xiao-Li HAN [1] Ping LI [1] Jing LIN [2]

[1] Institute of Acoustics, Chinese Academy of Sciences, Beijing, 100190, China
[2] State Key Laboratory for Manufacturing System Engineering, Xi'an Jiaotong University, Xi'an, Sha' anxi Province, 710049, China
[*] Corresponding author, E-mail: wuwentao@mail.ioa.ac.cn; Tel.: 86-010-82547723.

Ultrasonic virtual source imaging based on adaptive bi-directional point-wise focusing is proposed to improve the resolution and contrast when the depth increases. Firstly, ultrasonic array is divided into sub-arrays, the ultrasonic RF scanning lines are collected using fixed-focusing transmitting and receiving and these focuses are considered as virtual sources. Secondly, these scanning lines are point-wise focused using adaptive weighting, and then high-quality image is obtained. Simulations for point and speckle targets are used to verify this algorithm. It proves that when the F number is 1.5 and the focus is at 10 mm (such a sub-aperture corresponds to only 17 elements of array), the quality of images at different depths are consistent and equal to that of fixed-focus transmitting and dynamic receiving algorithm based on 64-channel imaging system. The experiment results prove that the image is much clearer on the whole by the proposed algorithm.

Keywords: Ultrasonic imaging; Virtual source; Bidirectional point-wise focusing

1. INTRODUCTION

Synthetic aperture ultrasonic imaging (SAUI) derives from synthetic aperture radar [1]. The frame rate, signal-to-noise-ratio (SNR) and contrast are improved by SAUI compared to conventional ultrasonic imaging. The SAUI system is not popularized because of higher requirements of hardware [2].

In order to overcome these shortcomings, C. Passmann and H. Ermert [3] proposed the virtual source (VS) synthetic aperture technology. Then C. H. Frazier [4] used the subaperture focusing to generate VS for improving SNR and resolution. M. H. Bae [5] used VS to make reconstruction of ultrasound image to improve the quality of image by linear array. Recently, J. Kortbek [6] proposed sequence beamforming and considered the virtual source reconstruction as the second beamforming process. M. Sutcliffe [7] applied VS in nondestructive testing. Researches on VS technology show that the typical performance between the algorithms of fixed-focusing transmitting and dynamic receiving and fully dynamic focusing can be obtained when the complexity of front-end hardware system is significantly reduced.

In conventional ultrasonic imaging of fixed-focus transmitting and dynamic receiving, high resolution can be only obtained near the focuses. The width of main lobe increases and the lateral resolution decrease as the depth of imaging increases. Although both transmitting and receiving focusing at the same time in whole plane can be implemented by SAUI and the relatively uniform resolution and contrast can be obtained, but the imaging speed is slow and SNR is low because each element transmits and receives in turn. Imaging algorithms based on VS was proposed for higher resolution and SNR. But at sometime, the low resolution scan lines based on VS can not be added coherently. To solve this problem, the adaptive bi-directional point-wise focusing method based on virtual source (BIPF-VS) which combining the VS imaging and coherent weighting is proposed in this paper. And in this algorithm the requirements of the front-end hardware are much lower than conventional ultrasonic imaging method and the lateral resolution and contrast are more consistent in the whole plane.

2. VIRTURAL SOURCE IMAGING

2.1 Bidirectional point-wise focusing imaging algorithm

978-1-4799-6425-3/14/$31.00 ©2014 IEEE

Fig. 1 shows the bi-directional point-wise focusing imaging algorithm based on VS. Three sub-apertures are marked in this figure and three corresponding focuses (VS) locate at A, B and C separately. The distance between two adjacent VS is d and the focal distance is z_f. The area covered by dashed line indicates the positions

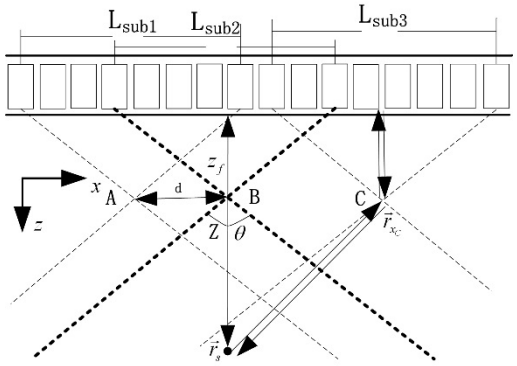

which can be reached by sub aperture L_{sub2} in the ray approximation.

Figure 1 bidirectional point-wise focusing imaging algorithm based on virtual source

Assuming a scatter exists in $\vec{r}_s$ (the coordinates is (x,z)) and locates in the center of sub-aperture L_{sub2}, the propagation time between the scatter and the VS B is:

$$t(\vec{r}_{x_B},\vec{r}_s)=2z/c=(2z_f\pm 2\left|z-z_f\right|)/c. \quad (1)$$

Without loss of generality, if a virtual source C locate at $\vec{r}_{xc}$ (the coordinates is (x_C, z_f)) and the lateral distance between the VS C and the VS B is Md, where M is an integer. The propagation time between the scatter and the VS C is:

$$\begin{aligned} t(\vec{r}_{x_C},\vec{r}_s)&=(2z_f\pm 2\left|\vec{r}_{x_C}-\vec{r}_s\right|)/c \\ &=(2z_f\pm 2\sqrt{(z-z_f)^2+(Md)^2})/c \end{aligned}, \quad (2)$$

In order to improve the resolution and contrast, all the scanlines of the virtual sources that cover this scatter are added, and then the synthesized signal at z is gotten as:

$$H(x,z)=\sum_{k=0}^{K(z)-1}W(x_k,z)S_{xk}(t(\vec{r}_{xk},\vec{r}_s)), \quad (4)$$

where the $H(x,z)$ is the high resolution image and $S_{xk}(z)$ is the low resolution scan line with the VS at (x_k,z_f). $K(z)$ is the number of VS covering this scatter, and $W(x_k,z)$ is the point-wise weighting coefficient of VS k located at (x_k,z_f). $t(\vec{r}_{xk},\vec{r}_s)$ is the propagation time between the scatter and the VS k.

Near the focus, only one scan line is added in the high resolution image, so the quality of imaging is equal to the conventional method. The imaging quality far away from the focus will be improved because the point farther away from the focus can be formed by more scan lines. The signs of the delays before and behind the focus are opposite, that's why the processing of superposition is called bidirectional point-wise focusing by Ref. 5.

2.2 Adaptive BIPF

The condition of higher resolution and SNR by BIPF is coherent superposition of low resolution images of the specific target signal. But this condition can not always be satisfied in practical application. Non-coherent superposition may lead to high side lobe level in none target area. Therefore, adaptive BIPF based on VS is proposed to reduce these pseudo sidelobes.

The spatial coherence factor (CF) is firstly proposed by K. W. Hollman [25]:

$$CF=\frac{(\sum_{m=0}^{N-1}\left|p(m)\right|)^2}{\sum_{m=0}^{N-1}\left|p(m)\right|^2}, \quad (4)$$

where $p(m)$ is the signal of element m after proper time delay. The CF is the ratio of coherent energy to total energy and can be used as coherence measurement of array signals.

So, the adaptive weighting coefficients are introduced into the BIPF:

$$H(x,z)=A(x,z)\sum_{k=0}^{K(z)-1}W(x_k,z)s_{x_k}(t(\vec{r}_{x_k},\vec{r}_s)), \quad (5)$$

where the adaptive weighting coefficients $A(x,z)$ is space variant and is used to enhance the coherent components and suppress the non-coherent components in the imaging.

3. SIMULATION

Simulations of point target imaging are done according to the theory of spatial impulse response. The lateral resolution and contrast of different algorithms are studied quantitatively. In all simulations, an ultrasonic linear array of 192 elements with center frequency of 3.5 MHz is used. Fixed-focusing imaging algorithm and dynamic focusing imaging algorithm are used to compare with the proposed algorithm. The element number of the aperture for fixed-focusing imaging algorithm and dynamic focusing imaging is 64 channels while that for the algorithms based on VS is dependent on F number.

Parameters of transducer and VS are listed in Table 1. The simulations with the focal distance of 5 mm, 10 mm and 20 mm, and F number of 0.5, 1 and 1.5 are included.

Four other algorithms are compared with the proposed algorithm to validate the performance. Algorithm 1 is dynamic-focusing transmitting and dynamic-focusing receiving (dynT-dynR); Algorithm 2 is fixed-focusing transmitting and dynamic-focusing receiving (fixT-dynR); Algorithm 3 is fixed-focusing transmitting and fixed-focusing receiving (fixT-fixR); Algorithm 4 is BIPF; Algorithm 5 is adaptive BIPF.

Table 1. Parameters of simulations

Parameters	*Symbol*	*Value (Unit)*
number of elements	M	192
Center frequency	f_0	3.5 MHz
Sampling frequency	F_s	40 MHz
Pitch	d	0.49 mm
Relative bandwidth	B	60%
Focal distance	Z_f	5mm, 10mm, 20mm
F number	$F_\#$	0.5, 1, 2
Maximum number of VS	N	91

Fig. 2 gives the images of point target using above five algorithms. In the center of these images there are 10 point targets with starting depth at 5 mm and axial interval of 10 mm.

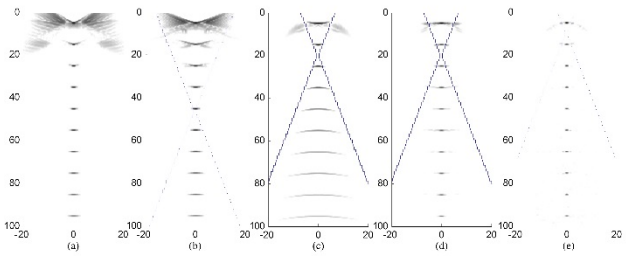

Figure 2 Images of point target by different algorithms (a) dynT-dynR (b) fixT-dynR (c) fixT-fixR (d) VS-BIPF, (e) VS-ABIPF

The imaging result of dynT-dynR algorithm by 64 channels sub-aperture is shown in Fig. 2(a). Due to fixed length aperture, high resolution is obtained in near field while decreases in far field. The imaging result of the fixT-dynR algorithm with F number equal to 1.5 and focus at 40 mm is shown in Fig. 2 (b). The highest resolution is obtained in the vicinity of the focus and become poor away from the focus. The imaging result of the fixT-fixR algorithm with F number equal to 1.5 and focus at 10 mm is shown in Fig. 2 (c). Obviously, the result is poorer than Fig. 2 (a) and Fig. 2 (b). The imaging result of the BIPF algorithm is shown in Fig. 4 (d). It can be seen that the resolutions at 10-70 mm are improved obviously. The image results of the ABIPF algorithm is shown in Fig. 4 (e). Compared with Fig. 4 (c) (d) (e), sidelobes can be reduced by adaptive weighting of ABIPF.

In order to further study the resolution of different algorithms quantitatively, -6 dB lateral widths at different depths are shown in Fig. 3. The consistent resolution can be gotten by BIPF algorithm and ABIPF algorithm and the best resolution is obtained by ABIPF algorithm.

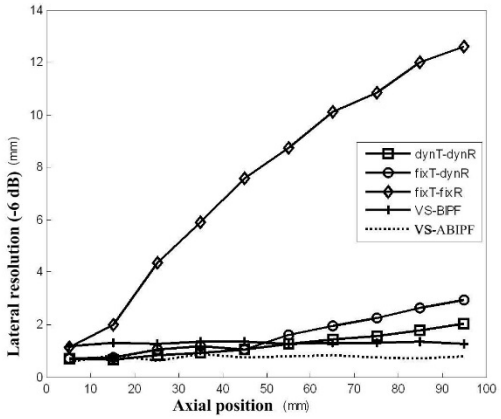

Figure 3 -6 dB lateral widths at different depth by different algorithms

Particularly, the VS-ABIPF number is 1.5 and the focal distance is 10 mm, so its effective aperture corresponds to only 17 elements. Compared to conventional imaging algorithm using 64 elements, equivalent performance is obtained by proposed algorithm using only 1/4 elements. The proposed algorithm can greatly reduce the complexity of hardware at front end.

4. EXPERIMENTS

In order to verify the performance of the proposed algorithm, the ultrasonic imaging system USCAS-32 (developed by Institute of Acoustics, Chinese Academy of Sciences) and the phantom KS107BD are used for imaging experiment. The USCAS-32 system can support 32 channels working independently at the same time. The maximum element number of probe array is 128. The beamformer supports fix-point focusing and dynamic focusing. The prebeamforming data can be collected, and then a variety of high resolution and high frame rate imaging algorithms can be studied based on this platform. Ultrasonic abdominal probe with radius of

curvature equal to 60 mm and center frequency at 3.5 MHz is used in this experiment.

Fig. 4 shows the results of three algorithms. The result of fixT-fixR is shown in Fig. 4(a). Although all the targets can be seen, the lateral expansion of point targets at deep and shallow position is very large. Especially, the resolution is poor from 10 mm to 40 mm. The result of BIPF with focus at 60 mm is shown in Fig. 10 (b). The resolution is greatly improved in the near field. The result of ABIPF with focus at 60 mm is shown in Fig. 10 (c). The resolution and contrast of the point target with depth less than 60 mm is obviously improved. But the point targets at the depths greater than 60 mm are improved slightly. It is because that the curvature of this array is 60 mm and beam divergence is led at large distance.

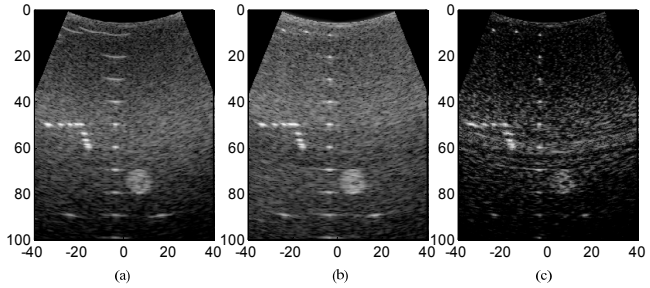

Figure 4 Imaging results (a) fixT-fixR (b) BIPF (c) ABIPF

5. CONCLUSION

In this paper, adaptive BIPF algorithm is proposed for solving the problem of the decreased resolution at deep depth. Bidirectional point-wise focusing based on VS and adaptive weighting are combined to improve the resolution and suppress sidelobes. The comparisons of the lateral resolution and contrast by simulation of point targets are used to verify the proposed ABIPF algorithm. Consistent resolutions at different depths can be obtained by ABIPF algorithm compared to the conventional fixT-dynR algorithm and dynT-dynR algorithm.

The imaging experiments using USCAS-32 system and KS107BD phantom are used to further validate that the high resolution and contrast can be obtained at different depth by ABIPF algorithm. And the hardware at front end by ABIPF algorithm is lower than conventional imaging system. When the F number is 1.5 and the focal length is 10 mm, the effective aperture is only 17 elements. According to the simulation, the image quality is equivalent to the conventional imaging algorithm with 64 elements.

Certainly, the complexity at back end is larger than conventional algorithms. In real time implementation of this algorithm, the high speed CPU or GPU can be used. This algorithm is attractive for its low complexity at front end.

In particular, the adaptive weighting of ABIPF algorithm is not limited to the coherent factor weighting. The adaptive coefficients can be extended to the generalized coherent factor, minimum variance beamforming or other adaptive weighting algorithms for different needs of imaging quality.

ACKNOWLEDGEMENTS

The work was supported by Chinese Academy of Sciences Institute of Acoustics Innovation Prospective Project (Y154211341).

REFERENCES

[1] Karaman M, Li PC, O'Donnell M. Synthetic aperture imaging for small scale systems. *IEEE Transactions on Ultrasonics, Ferroelectrics and Frequency Control*, 42(3): 429-442, 1995.

[2] Ylitalo J, Ermert H. Ultrasound synthetic aperture imaging: monostatic approach. *IEEE Transactions on Ultrasonics, Ferroelectrics and Frequency Control*, 41(3): 333-339, 1994.

[3] Passmann C, Ermert H. A 100-MHz ultrasound imaging system for dermatologic and ophthalmologic diagnostics, *IEEE Transactions on Ultrasonics, Ferroelectrics and Frequency Control*, 43(4): 545-552, 1996.

[4] Frazier CH, O'Brien WD. Synthetic aperture techniques with a virtual source element, *IEEE Transactions on Ultrasonics, Ferroelectrics and Frequency Control*, 45(1): 196-207, 1998.

[5] Bae MH, Jeong MK. A study of synthetic-aperture imaging with virtual source elements in B-mode ultrasound imaging systems, *IEEE Transactions on Ultrasonics, Ferroelectrics and Frequency Control*, 47(6): 1510-1519, 2000.

[6] Kortbek J, Jensen JA, Gammelmark KL. Sequential beamforming for synthetic aperture imaging, *Ultrasonics*, 53(1): 1-16, 2013.

[7] Sutcliffe M, Weston M, Charlton P, et al. Virtual source aperture imaging for non-destructive testing, *Insight-Non-Destructive Testing and Condition Monitoring*, 54(7): 371-379, 2012.

[8] Hollman K, Rigby K, O'Donnell M. Coherence factor of speckle from a multi-row probe. In: *Proc. IEEE UFFC Symp.*, pp. 1257—1260, IEEE, Lake Tahoe, NV, 1999.